J. Fluid Mech. (1984), *vol.* 143, *pp.* 429–449
Printed in Great Britain

Organized structures in turbulent Taylor–Couette flow

By A. BARCILON

Department of Meteorology and Geophysical Fluid Dynamics Institute, Florida State University, Tallahassee, Florida 32306

AND J. BRINDLEY

Department of Applied Mathematical Studies, University of Leeds, Leeds LS2 9JT

(Received 19 August 1983 and in revised form 15 February 1984)

A simple mathematical model is constructed to describe the regime of flow, extending over a wide range of values of Taylor number, in which turbulent Taylor–Couette flow in the annular region between two coaxial circular cylinders is characterized by the coexistence of steady coherent motion on two widely separated scales. These scales of motion, corresponding to the gap width of the annular region and to a boundary-layer thickness, are each identified as the consequence of a centrifugal instability, and are described as Taylor vortices and Görtler vortices respectively.

The assumption that both scales of motion are near marginal stability gives a closure to a pair of coupled eigenvalue problems, and the results of a linear analysis are shown to be in good agreement with many features of experimental observations.

1. Introduction

An earlier paper (Barcilon *et al.* 1979, subsequently referred to as BBLM) has reported observations, at very high values of the non-dimensional parameter that characterizes these flows, of an organized small-scale structure near the cylindrical walls in Taylor–Couette experiments. These experiments examined the behaviour of a fluid contained between two coaxial circular cylinders when the inner cylinder rotates at an angular speed Ω_1 while the outer one remains fixed. One of the important non-dimensional parameters in this problem is defined for a narrow-gap experiment as

$$T = R_1 \Omega_1^2 L^3/\nu^2 \tag{1.1}$$

and is called the (laminar) Taylor number in recognition of the important theoretical and experimental original contributions made by Taylor (1923) to this problem. In the above defining equation, R_1 is the inner radius, L is the gap width and ν is the (laminar) coefficient of kinematic viscosity. The sequence of flow behaviour observed as T is increased is discussed in some detail in BBLM, but it suffices to recall here that the transition from a state of no meridional motion to a state in which laminar toroidal vortices, called Taylor vortices, are first observed occurs when

$$T = T_c,$$

where T_c depends on the gap width and $T_c \approx 1700$ in the narrow-gap limit. Over a wide range of values of T such that $T_c < T < 400T_c$, a variety of wave-like perturbations disturbs the Taylor vortices, and much of the recent work on this parameter range has been well reviewed by DiPrima & Swinney (1981). However,

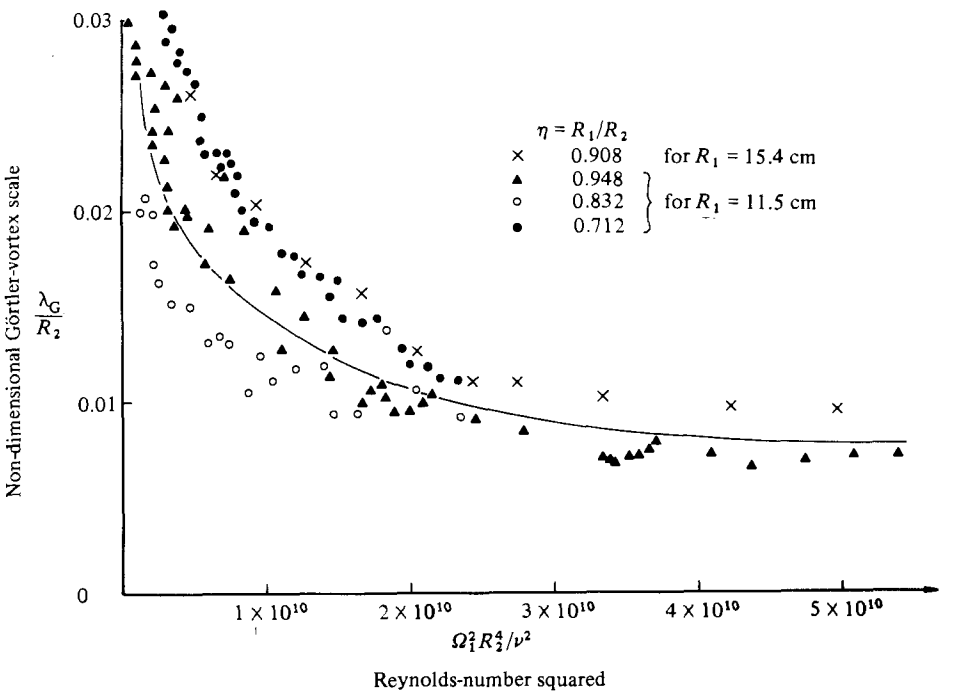

FIGURE 1. Ratio of scale of Görtler vortices to radius of curvature of wall for various gap widths. The scale is seen to depend only on Ω_1 and not on the Taylor number, which varies by two orders of magnitude at a given Ω_1 between the cases of narrowest and widest gap. Experiments performed by D. J. Quigley; theoretical prediction of this paper indicated by the solid line.

for $T/T_c \gg 400$, one observes steady turbulent structures which have many of the features of the laminar Taylor vortices. These structures, recognized in the flow-visualization photographs of BBLM by the axially periodic dark bands indicating radial inflow and outflow boundaries, are not wavy and exhibit a remarkable steadiness as T/T_c is increased over two or more orders of magnitude. A striking feature, not observed with the laminar Taylor vortices, is the presence, on the outer wall, of a fine pattern of streaks which tilt alternately at small angles $\pm\theta$ in neighbouring cells. This organized pattern was described by BBLM as 'herringbone' because of its appearance, and they conjectured that these streaks were the inflow and outflow of Görtler vortices (Görtler 1940) existing in the wall-boundary-layer region of the much larger Taylor circulation cells, and oriented along the helical streamlines of these cells, the pitch angle of which is measured by θ. The scale of the Taylor cells is commensurate with the gap width L between the rotating inner cylinder of radius R_1 and the outer stationary concentric cylinder of radius R_2.

Comparison of an elementary theory with experiments was made in BBLM, and subsequent experiments by Mobbs, using several different gap widths, have given similarly good agreement, supporting the original interpretation of the physical mechanism responsible for the small-scale streaks. We display this wider range of results in figure 1. Recent spectral results obtained by Mobbs are exemplified in figure 2; the marked dominance and containment near the wall of structures on the Görtler-vortex scale is very apparent.

The Görtler instability is of course a centrifugal instability, potentially occurring on a curved flow in which the circulation or local angular momentum decreases

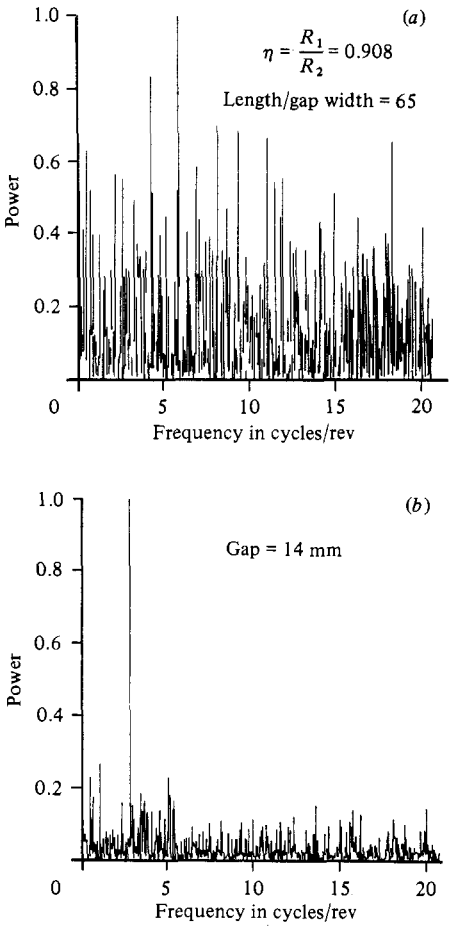

FIGURE 2. Frequency spectra obtained (*a*) at midgap and (*b*) 2 mm from the outer stationary cylinder at $T/T_c \sim 20000$, $L/R_1 \sim 0.1$. The very dominant frequency apparent in case (*b*) is presumed to correspond to the Görtler vortex streaks visible at this value of T.

outwards along the radius of curvature. The unstable modes or Görtler vortices described in the classical linear theory are tied to a rigid concave wall, the no-slip condition at which enforces such an outward decrease in circulation, and these vortices decay exponentially away from the wall. Thus no direct dependence on the gap width is expected in the occurrence and behaviour of Görtler vortices provided that the e-folding distance over which they decay is small compared with the gap width, and the observations at widely differing gap widths support this expectation; the existence and scale of the Görtler vortices depend only on the boundary curvature, together with the angular velocity Ω_1 of the inner cylinder, since at high values of the Taylor number, the mean azimuthal velocity is near to $\frac{1}{2}\Omega_1 R_1$ in a wide interior region away from the walls (see figure 3).

In experiments by Mobbs using low densities of aluminium particles for flow visualization, similar vortices are also seen on the *inner convex* wall, tilted in the sense opposite to that on the outer wall. The physical mechanism here is of course the same, since there is again a decrease in circulation, outwards along the radius of curvature, from the rotating inner cylinder to the interior region in which the mean azimuthal velocity is near to $\frac{1}{2}\Omega_1 R_1$.

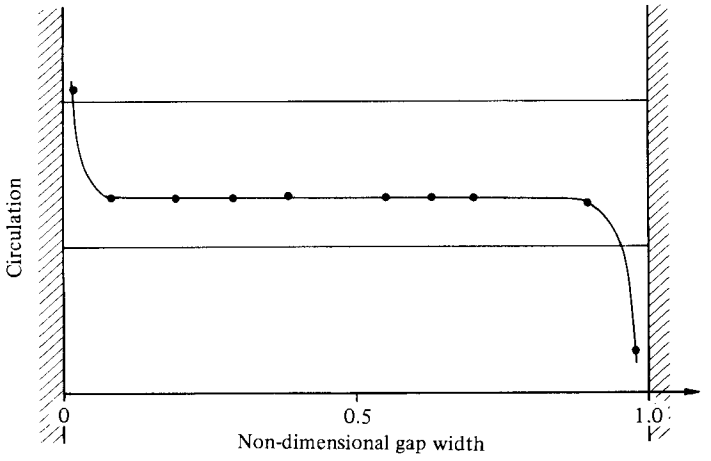

FIGURE 3. Variation of circulation ($r\overline{V}_0$ in our notation) with radius, schematically represented but based on observations of Taylor (1935), shown by solid circles, and many others.

In this paper we develop a consistent mathematical formulation, exploiting the wide separation of scales of the Taylor and Görtler modes, and isolate a pair of coupled eigenvalue problems for the existence of the two modes, together with equations satisfied by a mean (i.e. axially uniform) component of the flow field. For the flow far from the boundaries, i.e. in the 'Taylor' problem, we use a macroscopically averaged form of the Navier–Stokes equations, in which the averaging of the fine turbulent structure is parametrized by an eddy viscosity. Near the boundaries, by assuming a laminar steady state and linearizing about a mean swirl, we obtain equations similar to Görtler's original eigenvalue problem. The two stability problems are coupled through matched asymptotic expansions; the crucial assumption of marginal stability for both modes is required to 'close' the problem in the sense of providing a relationship between Reynolds stresses and mean profiles; it also enables us to use *linear* theory to make predictions of cell size, mean velocity profile, and torque transport. The good agreement with experimental results provides *a posteriori* justification of this assumption.

Perhaps the only striking observational feature upon which linear theory is unable to throw any light is the orientation of the herringbone pattern. However, the Görtler vortices are expected to lie along the total streamlines of the larger-scale Taylor-type structures, and the change of orientation with changing Taylor number is in good agreement with observed values of the amplitude of motion in the Taylor cells at high values of T. The decrease in the Taylor-cell amplitude with increasing Taylor numbers, as is shown in figure 4, suggests small tilts of the herringbone patterns away from a plane perpendicular to the rotation axis.

We expect that a prediction of the amplitude of Taylor cells, and hence of the orientation of the Görtler vortices, will require the development of weakly nonlinear theory pivoted about the results of this paper. Such a theory will, of course, be expected also to alter, to a small extent, the predicted values of our observations, but not to vitiate the excellent results of this linear theory. Our approach bears some resemblance to that adopted by Howard (1963) for the closely related problem of Rayleigh–Bénard convection at high values of the Rayleigh number, later developed by many workers into more formal upper-bound and optimum theories of turbulence and admirably surveyed by Busse (1978, 1981). The Taylor–Couette problem differs

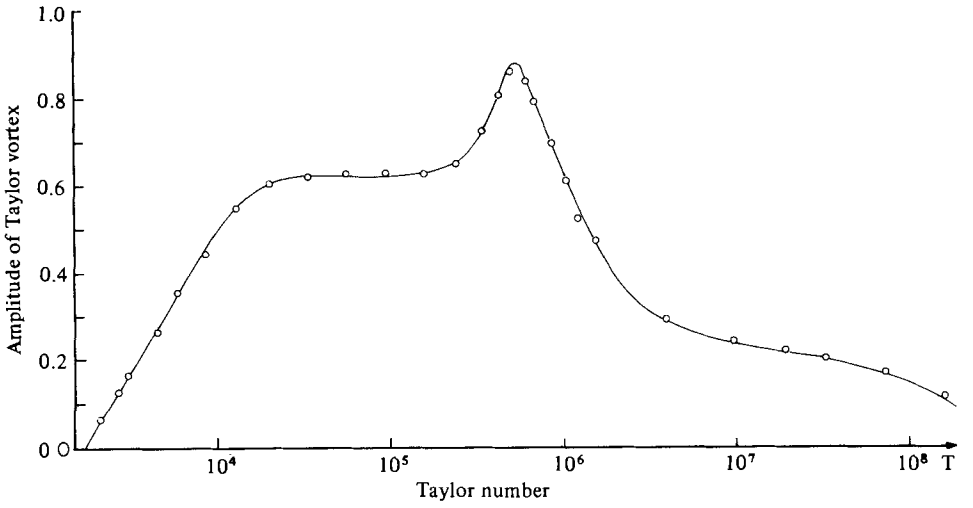

FIGURE 4. Amplitude of circulatory motion in Taylor vortices (after Bouabdallah & Cognet 1980). The amplitude is deduced from measurements of velocity gradients at the outer wall at different points of the Taylor cell.

from that of convection in a horizontal layer, or of turbulent channel flow, in its strong rotational symmetry constraint, forcing a definite orientation on both the Taylor- and Görtler-scale structures.

The mathematical formulation of the problem is given in §§2–5, and the solution to the linear problem is obtained in §6. In §7 we discuss the results in the context of observations made by a number of experimentalists.

2. Formulation of the problem

We wish to describe the dynamics of Taylor–Couette flow in long coaxial cylinders when the laminar Taylor number is 10^3 to 10^5 times the critical value for the onset of laminar Taylor vortices. At these high values of T, experiments do not suggest extreme sensitivity to end conditions, as is characteristic of laminar flows, and which creates great difficulties in predicting the precise axial wavenumber in purely laminar flow; instead we believe that there is no loss of reality in assuming infinite cylinders in the mathematical model.

It is appropriate to use cylindrical polar coordinates in which r is measured radially, ϕ azimuthally and z along the axis of the cylinder, so that the velocity field V has components (u, v, w) in these coordinate directions. Observations indicate that the flows are steady, i.e. the shape of the observed pattern does not appear to change appreciably with time; thus we shall assume that, in some averaged sense, we can let $\partial/\partial t = 0$.

We partition the total velocity field into mean and fluctuation fields, i.e. we write

$$\left.\begin{aligned} V &= \bar{V}(r) + V'(r, \phi, z), \\ p &= \bar{p}(r) + p'(r, \phi, z), \end{aligned}\right\} \tag{2.1}$$

where we define the $\bar{(\ )}$-average as

$$\bar{V}(r) = \lim_{l \to \infty} \frac{1}{2\pi l} \int_0^{2\pi} \mathrm{d}\phi \int_0^l V(r, \phi, \zeta)\, \mathrm{d}z, \tag{2.2}$$

and we have taken $\bar{V}' = 0$. We assume that $\bar{V}$ is entirely in the azimuthal (ϕ)-direction.

The equations for the mean and fluctuation fields are

$$\bar{V}\times(\nabla\times\bar{V})+\overline{V'\times(\nabla\times V')}-\tfrac{1}{2}\nabla(\bar{V}^2)-\tfrac{1}{2}\nabla(\overline{V'^2})=-\frac{1}{\rho}\nabla p+\nu\nabla\times(\nabla\times\bar{V}), \tag{2.3}$$

$$\bar{V}\times(\nabla\times V')+V'\times(\nabla\times\bar{V})-\nabla(\bar{V}\cdot V')=-\frac{1}{\rho}\nabla p'+\nu\nabla\times(\nabla\times V'). \tag{2.4}$$

It is useful to consider the azimuthal component of (2.3), which may be written in divergence form as

$$\overline{\frac{\partial}{\partial t}(r^2u'v')}=\nu\frac{\partial}{\partial r}\left(r^3\frac{\partial}{\partial r}\left(\frac{\bar{v}}{r}\right)\right), \tag{2.5}$$

which integrates to

$$2\pi\rho r^2\overline{u'v'}=2\pi\mu r^3\frac{\partial}{\partial r}\left(\frac{\bar{v}}{r}\right)-\tau, \tag{2.6}$$

where τ is the applied torque per unit length at $r = R_1$.

Since the flow is steady, the torque transport across all cylindrical surfaces must be the same and equal to τ; since $u' = 0$ at $r = R_1$, R_2, from (2.6) we see that the existence of a non-vanishing Reynolds-stress contribution $2\pi\rho r^2\overline{u'v'}$ to this torque transport at radial station r implies a steepening of the profile of $\bar{v}/r$ near the bounding cylinders. Indeed, the observed torque measurements, of the order of 100 times the laminar value (Quigley 1981; Smith & Townsend 1982), imply the existence of sharp boundary layers at $r = R_1$, R_2, in the mean azimuthal velocity field $\bar{v}$.

It will be convenient to introduce a stretched coordinate near the walls to describe the flow in these layers; we introduce a notation, to be defined more precisely later, of δ for a boundary-layer thickness, and $\overline{\mathscr{V}}$ for the mean-velocity field in the boundary layer.

Further progress is dependent on our ability to establish a second relationship between the Reynolds stresses and the mean velocity field, and the main concern of this paper is the proposal and test against experimental evidence of such a relationship, which is in effect a closure of the turbulent-flow problem (see e.g. Townsend 1976, p. 124).

We are guided by the approach and results of Malkus (1979); briefly, we expect the flow to be susceptible to two instability mechanisms, a shear instability, which relies on the presence of inflectional points in the velocity profile, and a centrifugal instability, which can arise when the radial gradient of circulation is negative. The local, instantaneous velocity profiles will contain inflectional points which will be the seat of shear-flow-type instabilities, albeit modified by rotational effects. However, in the spirit of Malkus (1979), we conjecture that there is a range of T within which these local shear instabilities conspire to produce a mean-velocity profile having no inflection points, and therefore immune from shear instability, but nevertheless exhibiting a circulation gradient which can be susceptible to centrifugal instabilities. Observations of the mean flows at very high Taylor number (see figure 3) support these ideas, and the results of Smith & Townsend (1982) suggest that this conjecture holds for $400T_c < T < 3\times10^5T_c$, but fails for greater values of T.

The actual form derived by Malkus for cylindrical Couette flow is

$$\bar{v}\approx\tan\left(\frac{\pi}{L}(r-\tfrac{1}{2}(R_1+R_2))\right). \tag{2.7}$$

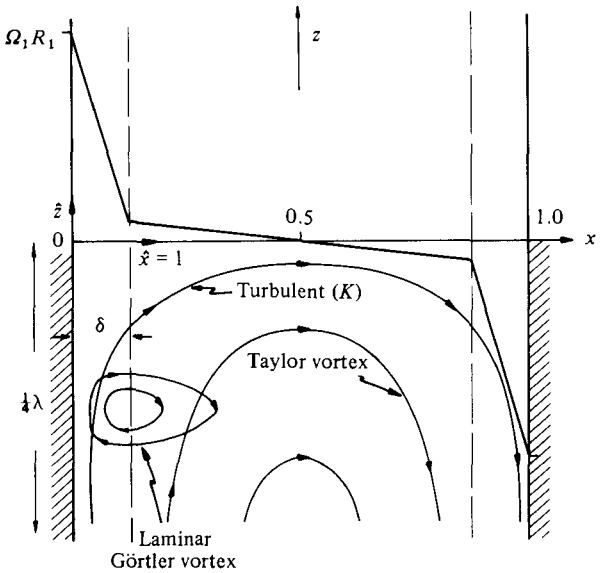

FIGURE 5. Schematic representation of the model examined in this paper. The sketched Görtler-vortex cell is the projection of the toroidal Görtler vortex onto the vertical plane. The vortex aligns its axis along the total helical streamline found on the outside of the larger toroidal vortex of the Taylor type. The intersection of the toroidal Görtler vortex near the $x = 1.0$ wall has not been shown.

This expression fails to satisfy the boundary conditions at $r = R_1$, R_2, and there is of necessity a (laminar) boundary layer at each wall. Our hypothesis is that a mean profile of this general form can support centrifugal instabilities on *two* separate scales L and δ associated with the interior region and with the boundary layer, respectively. The consequence of these instabilities is the existence in the interior region of a coherent, yet turbulent, cellular motion of the Taylor-vortex type, and in the boundary layers of a coherent laminar structure of the Görtler-vortex type. We effect the closure of the problem by requiring that each of these is a finite- (but small-) amplitude disturbance mode occurring in conjunction with a mean profile which is very nearly neutrally stable to such a mode.

This assumption enables us to proceed with an essentially linear analysis, though the model we adopt employs two parameters: δ, the boundary-layer thickness introduced earlier, and Γ, to be defined in (3.19), which is a measure of the mean circulation gradient in the interior region. These parameters are nonlinearly related through the requirement of marginal stability on the two scales. The form assumed for the mean flow is demonstrated schematically in figure 5.

3. The interior region

In developing the analysis, we first consider the interior motion, and partition the field V', defined in (2.1), into a part independent of ϕ, together with a part dependent on r, z and ϕ, writing

$$\left.\begin{aligned} V' &= \tilde{v}(r,z) + v'_{\mathrm{T}}(r,\phi,z). \\ p' &= \tilde{p}(r,z) + p'_{\mathrm{T}}(r,\phi,z). \end{aligned}\right\} \tag{3.1}$$

Thus $\tilde{v}(r,z)$ represents the field of the Taylor-vortex modes while $v'_{\mathrm{T}}(r,z)$ is the truly random fluctuation remaining after we subtract out $\bar{v}$ and $\tilde{v}$ from the total velocity

field. Observational evidence suggests that the lengthscale associated with $\boldsymbol{v}'_{\mathrm{T}}$ is much smaller than that of the Taylor vortices, and hence we can write down governing equations, obtained from (2.4) by using (3.1) and averaging over $0 \leqslant \phi \leqslant 2\pi$ and over a distance l in z, larger than the $\boldsymbol{v}'_{\mathrm{T}}$ scale but smaller than the $\tilde{\boldsymbol{v}}$-scale. We use the notation

$$\langle f(r,z)\rangle \equiv \frac{1}{2\pi l}\int_0^{2\pi} \mathrm{d}\phi \int_z^{z+l} f(r,\phi,z)\,\mathrm{d}z \tag{3.2}$$

for this average. We non-dimensionalize the equations by writing

$$x = \frac{r-R_1}{L} = a^{-1}\left(\frac{r}{R_1}-1\right), \tag{3.3}$$

by scaling all velocities by the inner wall velocity $\Omega_1 R_1$, and by scaling the pressure by $\rho\Omega_1^2 R_1^2$. Since the analysis that will follow is linear, it is unimportant that the perturbation velocities are not of order unity on this scale. We also make the small-gap approximation, i.e. we assume

$$\frac{\partial}{\partial r} \gg R_1^{-1}, \quad a \equiv \frac{L}{R_1} \ll 1. \tag{3.4}$$

Letting the non-dimensionalized quantities be represented by the same symbols as the dimensional quantities used until now, we write the non-dimensionalized equations as

$$\frac{\partial}{\partial x}(\tilde{u}^2)+\frac{\partial}{\partial z}(\tilde{u}\tilde{w})-2a\overline{V}\tilde{v} = -\frac{\partial p}{\partial x}+E\nabla^2\tilde{u}-\left\langle\frac{\partial}{\partial x}u_{\mathrm{T}}'^2\right\rangle-\left\langle\frac{\partial}{\partial z}u'_{\mathrm{T}}w'_{\mathrm{T}}\right\rangle, \tag{3.5}$$

$$\frac{\partial}{\partial x}(\tilde{u}\tilde{v})+\frac{\partial}{\partial z}(\tilde{w}\tilde{v})+\tilde{u}\frac{\mathrm{d}\overline{V}}{\mathrm{d}x} = E\nabla^2(\overline{V}+\tilde{v})-\left\langle\frac{\partial}{\partial x}u'_{\mathrm{T}}v'_{\mathrm{T}}\right\rangle-\left\langle\frac{\partial}{\partial z}v'_{\mathrm{T}}w'_{\mathrm{T}}\right\rangle, \tag{3.6}$$

$$\frac{\partial}{\partial x}(\tilde{u}\tilde{w})+\frac{\partial}{\partial z}(\tilde{w}^2) = -\frac{\partial\tilde{p}}{\partial z}+E\nabla^2\tilde{w}-\left\langle\frac{\partial}{\partial x}u'_{\mathrm{T}}w'_{\mathrm{T}}\right\rangle-\left\langle\frac{\partial}{\partial z}w_{\mathrm{T}}'^2\right\rangle, \tag{3.7}$$

$$\frac{\partial}{\partial x}\tilde{u}+\frac{\partial}{\partial z}\tilde{w} = 0, \tag{3.8}$$

where

$$\nabla^2 \equiv \frac{\partial^2}{\partial x^2}+\frac{\partial^2}{\partial z^2}, \quad E \equiv \frac{\nu}{\Omega_1 L R_1}, \tag{3.9}$$

and where, in the spirit of the Boussinesq approximation, we have let $a\to 0$ but retained aV in (3.5), at the same time neglecting aV compared with $\overline{V}_x$ in (3.6). We can regard (3.5)–(3.8) as the equations to be satisfied by a neutrally stable axisymmetric perturbation, described by $\tilde{\boldsymbol{v}}$ and $\tilde{p}$, to the mean-flow field $\overline{\boldsymbol{V}}(r)$, in the presence of small-scale fluctuations $\boldsymbol{v}'_{\mathrm{T}}$. In order to proceed, we need to make some assumption about the Reynolds stresses $\langle u'_{\mathrm{T}}v'_{\mathrm{T}}\rangle$ etc. appearing in these equations. It should be recognized that they are related to those described earlier in terms of $\overline{u'v'}$ by the equation

$$\overline{u'v'} = \tilde{u}\tilde{v}+\overline{u'_{\mathrm{T}}v'_{\mathrm{T}}} = \overline{\tilde{u}\tilde{v}}+\langle u'_{\mathrm{T}}v'_{\mathrm{T}}\rangle, \tag{3.10}$$

since we assume a large-scale uniformity of $\overline{u'v'}$. We exploit the separation of scales of the $\tilde{\boldsymbol{v}}$ and $\boldsymbol{v}'_{\mathrm{T}}$ fields to represent the momentum flux accomplished by the Reynolds stresses of the turbulent field ($'$) by an *eddy viscosity* K coupled to the gradients of the mean flow, i.e. we assume that

$$\left\langle\frac{\partial}{\partial x}u'_{\mathrm{T}}v'_{\mathrm{T}}\right\rangle = \overline{\frac{\partial}{\partial x}(u'_{\mathrm{T}}v'_{\mathrm{T}})} = -K\frac{\partial^2\bar{v}}{\partial x^2}, \tag{3.11}$$

where K is to be determined by the closure condition of marginal stability; it depends on the $\tilde{v}$-field, but we shall regard it as taking some suitable averaged value, recognizing that this is undoubtedly an idealization.

We can now introduce a stream function ψ such that

$$u = -\psi_z, \quad w = \psi_x. \tag{3.12}$$

Experiments (e.g. Bouabdallah & Cognet 1980; Smith & Townsend 1982) provide direct evidence that, at large T, the magnitude of meridional motion is a rapidly *decreasing* function of the magnitude of azimuthal motion, and we shall argue that small angles of the herringbone streaks provide indirect evidence of the small amplitude of the meridional motion. Thus we write

$$\left.\begin{aligned} \psi &= \epsilon\psi_1 + \epsilon^2\psi_2 + \ldots, \\ v &= \overline{V}_0 + \epsilon\tilde{v}_1 + \epsilon^2(\bar{v}_2 + \tilde{v}_2) + \ldots, \end{aligned}\right\} \tag{3.13}$$

where ϵ is a small parameter proportional in some sense to the tilt angle θ, which we have related to a measure of the Taylor vortex amplitude. Substituting (3.13) in (3.5)–(3.8) and eliminating the pressure to form a vorticity equation, we obtain, after linearizing with respect to the suffix-1 quantities, the following leading-order problem in ϵ:

$$2a\overline{V}_0\,\tilde{v}_{1z} = E_K\nabla^4\tilde{\psi}_1, \tag{3.14}$$

$$-\tilde{\psi}_{1z}\frac{\mathrm{d}\overline{V}_0}{\mathrm{d}x} = E\nabla^2\tilde{v}_1, \tag{3.15}$$

where

$$E_K = K/\Omega_1 LR_1. \tag{3.16}$$

The parameter E_K may be thought of as an eddy Ekman number which is related to an eddy Taylor number through

$$T_K = R_1\Omega_1^2 L^3/K^2. \tag{3.17}$$

In deriving (3.14) and (3.15), we have assumed $E \ll E_K$ and

$$\nabla^2\overline{V}_0 = 0, \tag{3.18}$$

consistent with our representation of the basic state in the interior region by

$$\overline{V}_0(x) = \tfrac{1}{2} - \Gamma(x - \tfrac{1}{2}), \tag{3.19}$$

where Γ is as-yet unknown.

In anticipation of the smallness of Γ, the result of substituting (3.19) into (3.14) and (3.15) is

$$a\tilde{v}_{1z} = E_K\nabla^4\tilde{\psi}_1, \tag{3.20}$$

$$\Gamma\tilde{\psi}_1 = E_K\nabla^2\tilde{v}_1, \tag{3.21}$$

which give, upon eliminating $\tilde{v}_1$,

$$\nabla^6\tilde{\psi}_1 - \left(\frac{a\Gamma}{E_K^2}\right)\tilde{\psi}_{1zz} = 0. \tag{3.22}$$

The quantity $a\Gamma/E_K^2$, which will appear later as an eigenvalue of the boundary-value problem, may be written in terms of the *laminar* Taylor number T as

$$\frac{a\Gamma}{E_K^2} = \Gamma T\left(\frac{\nu}{K}\right)^2.$$

We have considered in the Appendix the effect of retaining the $O(\Gamma)$ terms in (3.14) and (3.15); their neglect appears to be well justified.

4. The boundary-layer region

The boundary layer found on the $x = 0$ wall has a basic velocity field, denoted by $\mathscr{V}(x, z)$, which at the 'edge' of that layer must match the sum of the interior $\overline{V}_0$ and $\tilde{v}_1$, $\tilde{\psi}_1$ fields. Note that the z-component of $\mathscr{V}$ alternates in sign between adjoining Taylor vortices in the interior flow. Superposed on the basic field we assume the existence of a perturbation field $\hat{\boldsymbol{v}}$, constituting the Görtler vortices, which, we conjecture, arise as an instability of the basic field.

It is advantageous to discuss the dynamics of the boundary layer in terms of an intrinsic coordinate system in which the z- and ϕ-coordinate directions are replaced by coordinate directions $\hat{\eta}$ along the total streamline direction of $\mathscr{V}$, and $\hat{\zeta}$ normal to that direction. This system is tilted at an angle θ to the (ϕ, z)-system, and we assume that

$$\theta \sim \tan\theta \sim \frac{\tilde{\psi}_{1x}(0, z)}{\overline{V}_0(0)}, \tag{4.1}$$

consistent with the matching condition at the edge of the boundary layer.

If we introduce stretched intrinsic coordinates, based on a boundary-layer thickness δ, so that

$$\hat{x} = x/\delta, \tag{4.2}$$

this matching condition is

$$\mathscr{V}(\infty, z) = (\overline{V}_0(0) + \tilde{v}_1(0, z) + \ldots, \tilde{\psi}_{1z}(0, z) + \ldots). \tag{4.3}$$

The other new coordinates are

$$\left.\begin{aligned} \hat{\eta} &= \frac{y}{\delta}\cos\theta + \frac{z}{\delta}\sin\theta, \\ \hat{\zeta} &= -\frac{y}{\delta}\sin\theta + \frac{z}{\delta}\cos\theta, \end{aligned}\right\} \tag{4.4}$$

and the components of the perturbation velocity field $\hat{\boldsymbol{v}}$ are related to $\boldsymbol{V}'$ of (3.1) by

$$\left.\begin{aligned} \hat{u} &= \frac{\delta}{E}u', \\ \hat{v} &= v'\cos\theta + w'\sin\theta, \\ \hat{w} &= -v'\sin\theta + \omega'\cos\theta. \end{aligned}\right\} \tag{4.5}$$

Following, for example, Hammerlin (1956), we may write the linearized equations for the stability of longitudinal Görtler vortices in the form

$$\left.\begin{aligned} \left(\frac{\partial^2}{\partial\hat{x}^2} + \frac{\partial^2}{\partial\hat{\zeta}^2}\right)\hat{v} &= \hat{u}\frac{\partial\mathscr{V}}{\partial\hat{x}}, \\ \left(\frac{\partial^2}{\partial\hat{x}^2} + \frac{\partial^2}{\partial\hat{\zeta}^2}\right)\hat{u} &= -2G_{(\delta)}\mathscr{V}\frac{\partial^2\hat{v}}{\partial\hat{\zeta}^2}, \end{aligned}\right\} \tag{4.6}$$

where $\mathscr{V}$ is the magnitude of $\mathscr{V}$ and $G_{(\delta)}$ is a Görtler number defined by

$$G_{(\delta)} \equiv \frac{\delta^3 a}{E^2 R} = \frac{\Omega_1^2 R_1^2 L^2 \delta^2}{\nu^2}\frac{L\delta}{R_1 R} \tag{4.7}$$

and based on the non-dimensional radius of curvature $R(=1+O(\theta^2))$ of the streamline of the total velocity $\mathscr{V}$. As boundary conditions we require that

$$\left(\hat{u}, \hat{v}, \frac{\partial \hat{u}}{\partial \hat{x}}\right) = 0 \quad \text{at} \quad \hat{x} = 0, \infty. \tag{4.8}$$

The above eigenvalue problem was first considered by Görtler (1940), then by Meksyn (1950), and in greater detail by Hammerlin (1956), who calculated the marginal curve for six velocity profiles, and found that his results were insensitive to details of the basic state profile. The profile

$$\mathscr{V} = \left\{ \begin{array}{ll} \hat{x} & (0 \leqslant \hat{x} \leqslant 1), \\ 1 & (\hat{x} > 1) \end{array} \right\} \tag{4.9}$$

was one of the six considered by Hammerlin as well as Meksyn. The Görtler number was defined in these problems in terms of a momentum thickness δ_2, where

$$\delta_2 \equiv \delta \int_0^\infty \mathscr{V}(1-\mathscr{V})\, \mathrm{d}\hat{x},$$

which gives $\delta_2 = \frac{1}{6}\delta$ for the profile (4.9). Hammerlin's calculations showed that:

(i) the minimum critical Görtler number was fairly insensitive to the exact shape of the profile and that

$$G_{(\delta_2)\mathrm{c}} \approx 0.09, \tag{4.10}$$

or

$$G_{(\delta)\mathrm{c}} \approx (0.09)\, 6^3 \approx 19,$$

where we have denoted by a suffix c the minimum critical value;

(ii) the minimum critical Görtler number occurred for wavelengths large compared with δ_2: the critical wavelength λ_G for $\delta/R \sim 10^{-4}$ was shown by Hammerlin to be near $40\pi\delta_2$;

(iii) the velocity profiles, when plotted against the coordinate $\hat{x}$, normal to the boundary, were close to their maximum value when $\hat{x} = 1$, i.e. when the basic-state velocity $\mathscr{V}$ had reached its freestream value.

There is some disagreement in the literature over the appropriate value for $G_{(\delta)\mathrm{c}}$, and in making comparison with experiments we have used the value $G_{(\delta_2)\mathrm{c}} = 0.36$, with a concomitant change in the value of λ_G to about $15\pi\delta_2$, which appears to represent the consensus of opinion (Meksyn 1961; Smith 1955; Bippes 1972; Floryan & Saric 1982). Very recent work by Hall (1982, 1983) has stressed the deficiencies of many of these theories and has pointed to the importance, in the classical growing-boundary-layer problem, of the non-parallel nature of the flows and the dependence on distance from the leading edge. Substantial changes in G_c were noted by Hall, and we are conscious of the uncertainty surrounding the precise values to be used in this somewhat different problem, of which a detailed study seems worthwhile. However, the dependence of the experimentally measurable quantities on G_c is weak, at worst on the $\frac{1}{3}$ power.

5. Boundary and matching conditions

We have already required that the Görtler solution satisfies the no-slip condition at the rigid boundary found at $\hat{x} = 0$. Also the small-scale fluctuating motions due to the Görtler vortices vanish as $\hat{x} \to \infty$. We must now provide a set of matching conditions between the laminar Görtler region and the turbulent Taylor-vortex

region. Because of the insensitivity of the dynamics in the Görtler layer to the exact choice of a basic-state velocity profile in that region, we choose the simplest velocity profile and require that

$$\mathscr{V} = \begin{cases} \frac{1}{2}(\Gamma-1)\hat{x}+1 & (0 \leqslant \hat{x} \leqslant 1), \\ \overline{V}_0(0)\sec\theta & (\hat{x} > 1), \end{cases} \tag{5.1}$$

where, from (3.19),

$$\overline{V}_0(x) = \tfrac{1}{2}(1+\Gamma)-\Gamma x, \quad x = \delta\hat{x}. \tag{5.2}$$

Matching at $\hat{x} = 1$ gives, on requirement of

(*a*) continuity of velocity parallel to the interface

$$\begin{aligned} \mathscr{V}(1,z)\cos\theta &= \overline{V}_0(0)+\tilde{v}_1(0,z), \\ \mathscr{V}(1,z)\sin\theta &= \tilde{\psi}_{1x}(0,z); \end{aligned} \tag{5.3}$$

(*b*) continuity of tangential stress

$$\begin{aligned} \cos\theta\left(\frac{E}{\delta}\frac{\partial\mathscr{V}}{\partial\hat{x}}-\langle\tilde{u}\tilde{v}\rangle\right)\Big|_{\hat{x}=1} &= E_K\left(\frac{\mathrm{d}\overline{V}_0}{\mathrm{d}x}+\frac{\partial\tilde{v}_1}{\partial x}\right)\Big|_{x=0}, \\ \sin\theta\left(\frac{E}{\delta}\frac{\partial\mathscr{V}}{\partial\hat{x}}-\langle\tilde{u}\tilde{v}\rangle\right)\Big|_{\hat{x}=1} &= E_K\left(\frac{\partial^2\tilde{\psi}_1}{\partial x^2}+\frac{\partial^2\tilde{\psi}_1}{\partial z^2}\right)\Big|_{x=0}, \end{aligned} \tag{5.4}$$

(*c*) continuity of mass flux

$$\hat{u}(1,\zeta,z) = \tilde{\psi}_{1z}(0,z); \tag{5.5}$$

and we can now use the more specific definition

$$\langle f\rangle \equiv \frac{1}{l_G}\int_z^{z+l_G} f\,\mathrm{d}z, \tag{5.6}$$

where l_G is the Görtler-vortex scale.

To leading order we get

$$\frac{E}{\delta}\left(\frac{\partial\mathscr{V}}{\partial\hat{x}}\right)\Big|_{\hat{x}=1} = E_K\left(\frac{\mathrm{d}\overline{V}_0}{\mathrm{d}x}\right)\Big|_{x=0}, \tag{5.7}$$

$$-\langle\tilde{u}\tilde{v}\rangle|_{\hat{x}=1} = E_K\left(\frac{\partial\tilde{v}_1}{\partial x}\right)\Big|_{x=0}, \tag{5.8}$$

$$\theta\frac{E}{\delta}\left(\frac{\partial\mathscr{V}}{\partial\hat{x}}\right)\Big|_{\hat{x}=1} = E_K\frac{\partial^2\tilde{\psi}_1}{\partial x^2}\Big|_{x=0}, \tag{5.9}$$

$$\tilde{\psi}_1(0,z) = 0. \tag{5.10}$$

Finally taking an $\overline{(\ )}$-average of (5.2) and subtracting that result from (5.2) gives

$$\tilde{v}_1(0,z) = 0. \tag{5.11}$$

6. Leading-order solution

In the interest of clarity let us summarize the statement of the problem. The Taylor-vortex problem is governed by (3.22), (3.12), (3.20), (5.11), (5.10) and (5.9), which may be written as

$$\nabla^6\tilde{\psi}_1-\frac{a\Gamma}{E_K^2}\tilde{\psi}_{1zz} = 0, \tag{6.1}$$

where

$$\tilde{u}_1 = \tilde{\psi}_{1z}, \quad \tilde{w}_1 = \tilde{\psi}_{1x}, \tag{6.2}$$

$$\tilde{v}_{1x} = \frac{E_K}{a}\nabla^4\tilde{\psi}_1, \tag{6.3}$$

subject to the boundary conditions

$$\tilde{v}_1(0,z) = \tilde{v}_1(1,z) = 0,$$

i.e.

$$\left.\frac{\partial^4\tilde{\psi}_1}{\partial x^4}\right|_{x=0,1} = 0, \tag{6.4}$$

$$\tilde{\psi}_1(0,z) = \tilde{\psi}_1(1,z) = 0, \tag{6.5}$$

$$\tilde{\psi}_{1xx}(0,z) = \frac{\Gamma-1}{\Gamma+1}\frac{\nu}{K\delta}\tilde{\psi}_{1x}(0,z). \tag{6.6}$$

In deriving (6.6) from (5.9), we have used (4.2) and (5.1). A similar condition to (6.6) holds at $x = 1$.

The basic state consists of

$$\left.\begin{aligned} \mathscr{V} &= 1+\tfrac{1}{2}(\Gamma-1)\hat{x}_{\mathrm{L}} \quad (0 \leqslant \hat{x}_{\mathrm{L}} \leqslant 1), \\ \overline{V}_0 &= \tfrac{1}{2}(1+\Gamma)-\Gamma x \quad (0 \leqslant x \leqslant 1), \\ \mathscr{V} &= \tfrac{1}{2}(\Gamma-1)\hat{x}_{\mathrm{R}} \quad (-1 \leqslant \hat{x}_{\mathrm{R}} \leqslant 0), \end{aligned}\right\} \tag{6.7}$$

where $\hat{x}_{\mathrm{L}}$ and $\hat{x}_{\mathrm{R}}$ are the stretched variables on the left and right boundaries. Continuity of stress in the basic state requires that, from (5.7),

$$\frac{1}{2}\frac{\nu}{K\delta}(1-\Gamma) = \Gamma, \tag{6.8}$$

together with a similar condition near the $x = 1$ boundary. In these equations we do not know δ, Γ, K and therefore E_K.

Using (6.8) in (6.6) we find that the latter simplifies to

$$\tilde{\psi}_{1xx}(0,z)+\frac{2\Gamma}{1+\Gamma}\tilde{\psi}_{1x}(0,z) = 0. \tag{6.9}$$

Observational evidence seems to point to the smallness of Γ; thus, if we drop the term $O(\Gamma)$, (6.9) approximates to

$$\tilde{\psi}_{1xx}(0,z) = 0. \tag{6.10}$$

Equations (6.10), (6.4), (6.5) and (6.1) constitute the classical free–free Rayleigh–Bénard convection problem (Chandrasekhar 1961). We can at once write that the minimum critical value of the parameter entering (3.22) is

$$\frac{a^2}{E^2}\left(\frac{E^2}{E_K^2}\right)\Gamma_{\mathrm{c}} = T\Gamma_{\mathrm{c}}\left(\frac{\nu}{K_{\mathrm{c}}}\right)^2 = \tfrac{27}{4}\pi^4, \tag{6.11}$$

where the subscript c denotes a quantity at its critical value. The critical non-dimensional wavenumber associated with that problem is

$$\frac{\pi}{\sqrt{2}} \approx 2.22. \tag{6.12}$$

The problem described by (4.6), (4.7) and (4.8) is exactly the problem considered by Görtler and others, except that the mainstream flow has a magnitude $\frac{1}{2}\Omega_1 R_1 (1-\Gamma)$ instead of unity; the appropriate Görtler number for this problem is then

$$G'_{(\delta)} = \frac{(\frac{1}{2}(1-\Gamma)\,\Omega_1 R_1 L\delta)^2}{\nu^2}\frac{L\delta}{R_1 R}.$$

If we take the maximum critical value of $G'_{(\delta)\mathrm{c}} \approx 76$ we get

$$\frac{\delta^3 a}{E^2} = G_{(\delta)\mathrm{c}} \approx \frac{76}{\frac{1}{2}(1-\Gamma)^2}, \tag{6.13}$$

where we have assumed that R, the normalized radius of curvature, is unity, and have taken the larger value of $G_{(\delta_2)\mathrm{c}}$ mentioned in §4.

If we demand that each flow structure is close to marginal stability, we obtain from (6.13) the critical thickness

$$\delta_\mathrm{c}^3 = \frac{E^2}{a} G_\mathrm{c} = \frac{G_\mathrm{c}}{T},$$

i.e.

$$\delta_\mathrm{c} = G_\mathrm{c}^{\frac{1}{3}} T^{-\frac{1}{3}}, \tag{6.14}$$

while from (6.4) we obtain a relationship between Γ and E_K. From (5.7)

$$\left(\frac{\nu}{K}\right)_\mathrm{c} = 2\delta_\mathrm{c}\frac{\Gamma_\mathrm{c}}{1-\Gamma_\mathrm{c}} \approx 2\delta_\mathrm{c}\Gamma_\mathrm{c}. \tag{6.15}$$

Using the above expression in (6.11) we obtain

$$\Gamma_\mathrm{c} \approx \left(\frac{27\pi^4}{16 G_\mathrm{c}^3}\right)^{\frac{1}{3}} T^{-\frac{1}{9}}, \tag{6.16}$$

and using (6.16) in (6.15) we get

$$\left(\frac{\nu}{K}\right)_\mathrm{c} \approx 2\left(\frac{27\pi^4 G_\mathrm{c}^{\frac{1}{3}}}{16}\right)^{\frac{1}{3}} T^{-\frac{4}{9}}. \tag{6.17}$$

Another quantity that can be measured is the torque; in dimensional form the torque $\mathscr{G}_*$ per unit length of the cylinder

$$\mathscr{G}_* = \frac{\pi\Omega_1 R_1^3 \mu}{L}\frac{1-\Gamma}{\delta_\mathrm{c}},$$

i.e.

$$\mathscr{G}_* = \frac{\pi\Omega_1 R_1^3 \mu}{L} G_\mathrm{c}^{-\frac{1}{3}} T^{\frac{1}{3}}(1-\Gamma). \tag{6.18}$$

Equations (6.11), (6.14), (6.16), (6.17) and (6.18) constitute the main results of this investigation. All these quantities, with the exception of $(\nu/K)_\mathrm{c}$, are measurable, implicitly or explicitly, and in §7 we comment on the relationships of predicted to observed values.

7. Discussion and conclusions

In constructing this model we have assumed

(i) inhomogeneous turbulent shear flow with boundary layers at the cylindrical walls (based on *all* experimental evidence);

(ii) that inflexional instabilities create a mean profile which is itself immune from further inflectional instability;

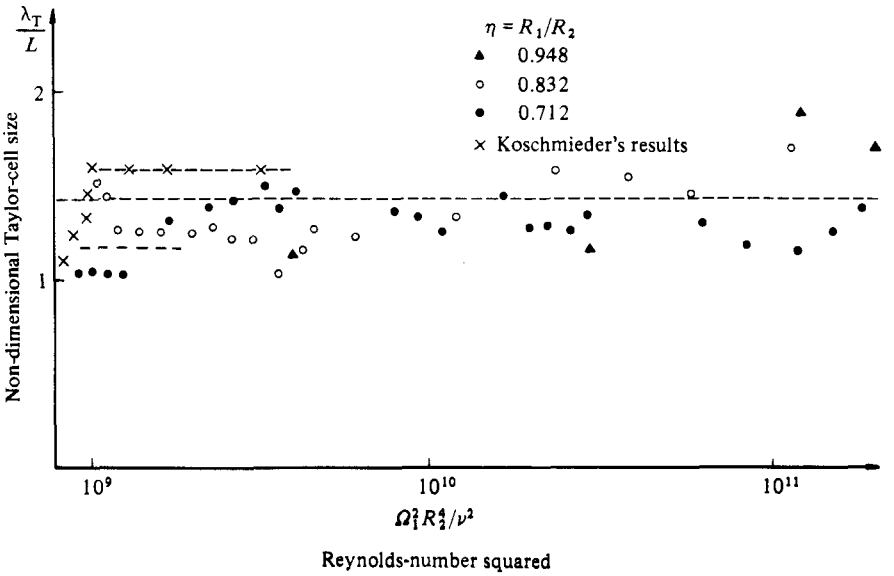

FIGURE 6. Scale of Taylor cells relative to gap width observed in experiments with varying gap widths. Experiments performed by D. J. Quigley; results of Koschmieder (1979) also indicated; theoretical prediction indicated by middle dashed line. Experimental results of Koschmieder (1979) indicated by upper dashed line (steady increase in Ω experiments) and lower dashed line (sudden-start experiments).

(iii) that the resulting profile might nevertheless be susceptible to centrifugal instability;

(iv) that this profile might be modelled by straight-line segments in the (turbulent) interior and in the (laminar) boundary layers;

(v) that each of these segments is marginally stable to centrifugal instabilities, represented respectively by modes of Taylor-vortex and Görtler-vortex type;

(vi) that the transport of torque across the channel may be modelled by an appropriate viscosity coupled to the mean flow and that in the interior the mean flow is coupled to an eddy viscosity parametrizing the Reynolds stresses of the fluctuating fields.

It seems to us that assumption (i) is amply justified without further comment, that (iv) and (vi) are in the nature of approximations to the true situation, but are not crucial to the *qualitative* merit of the model, but that (ii), (iii) and (v) are hypotheses of major importance, which enable us to close the problem mathematically, and which are to be tested by comparison of predictions with observations. A number of features predicted in §6 may be so compared; it is convenient to review them systematically.

7.1. *Scale of Taylor cells*

We noted in §4 that the boundary-value problem for the Taylor cells is identical (in this limit of small gap-width/radius ratio) to the problem of Rayleigh–Bénard convection in a horizontal layer bounded by stress-free horizontal surfaces – the so-called free–free problem. The horizontal wavelength of the convection rolls predicted by linear theory in that well-known problem is $\sqrt{2}$ times the layer thickness. Observations by Koschmieder (1979) and other workers including Mobbs provide supportive experimental evidence for this scale. In figure 6 we have assembled relevant observations from a number of workers; the comparison with the predicted value is seen to be good.

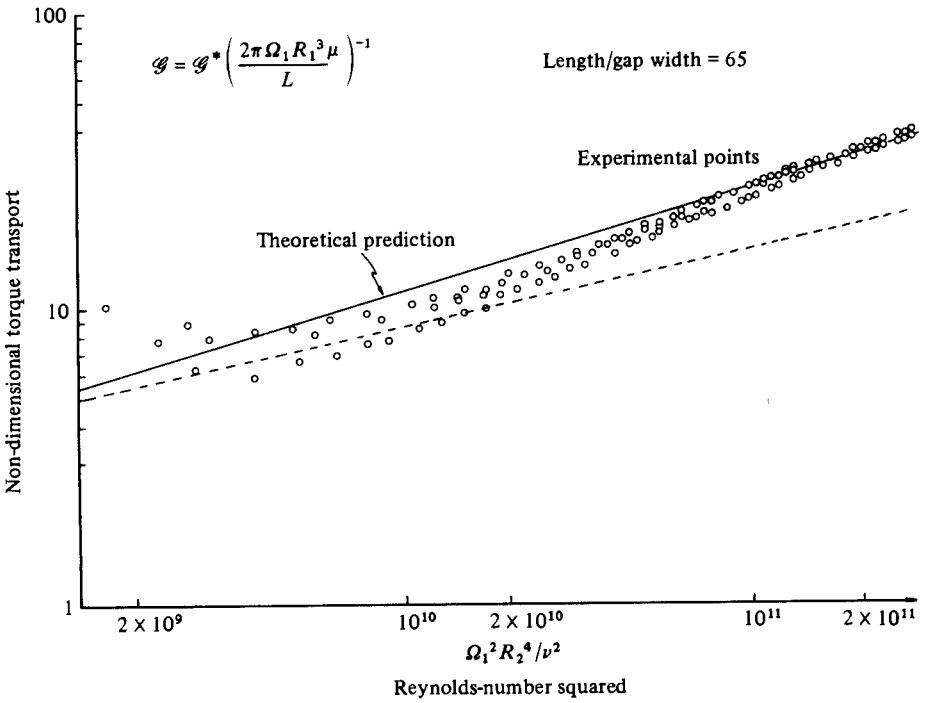

FIGURE 7. Non-dimensional torque transport measured in experiments performed by D. J. Quigley in long annulus with $L/R_1 \sim 0.1$. Theoretical predictions (based on (6.18) and (6.13)) indicated by solid line representing the expression

$$\mathscr{G} = \frac{1}{2}\left(\frac{\Omega_1^2 R_1^4}{\nu^2}\right)^{\frac{1}{3}} G_{(\delta)c}^{-\frac{1}{3}}\left(\frac{L}{R_1}\right);$$

Batchelor's (1960) prediction has the form

$$\mathscr{G} = A\left(\frac{\Omega_1^2 R_1^4}{\nu^2}\right)^{\frac{1}{4}}\left(\frac{L}{R_1}\right)^{\frac{3}{4}},$$

where A is an unknown constant, certainly less than 0.5 and possibly $O(10^{-1})$. For comparison we indicate by a dashed line this expression for the (arbitrary) value $A = 0.2$.

7.2. *Torque transport*

Expression (6.18) for the torque, viz

$$\mathscr{G}_* \approx \frac{\pi\Omega_1 R_1^3 \nu}{L} G_c^{-\frac{1}{3}} T^{\frac{1}{3}}, \tag{7.1}$$

is seen to vary as $\Omega_1^{\frac{5}{3}}$ with increasing Ω_1.

It is interesting that the model for high-Taylor-number flow proposed by Batchelor (1960), based on the conjecture that a laminar boundary-layer flow in the meridional velocity component surrounding the Taylor cell is present, predicts a variation as $\Omega_1^{\frac{3}{2}}$ for large Ω_1. It appears that the model proposed here permits a larger torque transport. Comparison with torque measurements (Brindley, Mobbs & Quigley 1981) is good for large Ω_1 (figure 7). This accuracy of the linear theory is compatible with the observations of Bouabdallah & Cognet (1980) showing a decreasing Taylor-cell amplitude for increasing Ω_1 (figure 4).

7.3. *Internal circulation gradient*

No systematic series of experiments has provided values of Γ to compare with the value of Γ predicted in (6.16), which implies that $\Gamma \sim \Omega_1^{-\frac{2}{3}}$. However, all experimental results (e.g. Smith & Townsend 1982; Taylor 1935) support the qualitative form of the mean gradient we have assumed. In the above theory we have of course, assumed the torque transport across the interior to be accomplished solely by the mean flow; the amplitude of the Taylor vortex has effectively been taken to be zero. A more realistic model should take account of the torque transport accomplished by Reynolds stresses associated with a finite-amplitude Taylor cell, with a consequent reduction in the value of Γ, and of the effects of finite gap width. It is however worthwhile to examine *a posteriori* the consequences of taking into account the finite value of Γ predicted; this we do in the Appendix.

7.4. *Scale of Görtler vortices*

We have already commented in BBLM and in §1 on the excellent agreement between prediction and experiment (figure 1). It is particularly noteworthy that the predicted non-dimensional scale

$$\frac{\lambda_G}{R_2} \approx \frac{6\pi L\delta_2}{R_2} \propto G_c^{\frac{1}{3}} \left(\frac{\Omega_1^2 R_2^4}{\nu^2}\right)^{-\frac{1}{3}} \tag{7.2}$$

is independent of gap width. The observational results illustrated, based on four widely differing gap widths, collapse very closely on to the predicted curve (figure 1), showing convincingly that the observed phenomenon is independent of gap width, and depends only on 'mainstream velocity' $\frac{1}{2}\Omega_1 R_1$ and curvature R_2. The values of Taylor number for the cases illustrated vary by a factor of nearly 200 for the same value of Ω_1.

7.5. *Orientation of Görtler vortices*

We cannot expect our linear theory to give any information on this, as the orientation depends on the amplitude of the Taylor-cell motion. However, we can compare (figure 8) observations of the orientation for varying Ω_1 with observations of Taylor-cell amplitude at large Taylor number (Boubdallah & Cognet 1980). There is clearly no evidence here to invalidate the assumption that the streak orientation measures the direction of the total velocity in the Taylor-cell motion.

As the orientation varies, the radius of curvature R also varies, in which case, using the definition of G_c in (4.10), it is clear that $\delta \sim \Omega_1^{-\frac{2}{3}} R^{\frac{1}{3}}$. This is of course maximized by minimizing R, which means reducing θ, the result of which is that the length of the individual Görtler vortices is increased. Now, a well-known consequence of the presence of longitudinal vortex structures in turbulent spots arising in wall boundary layers is the evolution of longitudinal flow profiles having points of inflection (e.g. Blackwelder & Eckelmann 1979). These profiles arise as a consequence of the sweeping of low-velocity fluid away from the wall by a pair of adjacent counter-rotating vortices. We might then conjecture that, at still higher Taylor numbers, the lengthening of the Görtler vortices could lead locally to an inflectional instability mechanism of this kind, which would disrupt the organized, coupled structures described here, and result in a flow more nearly like a turbulent channel flow in its character. Experiments at higher values of T (Smith & Townsend 1982), carried out since a first version of this paper was written, appear to bear out this conjecture.

Before concluding, a comment on the stability of our first-order model might be useful. Thus, although we have *assumed* that the mean profile remains near that

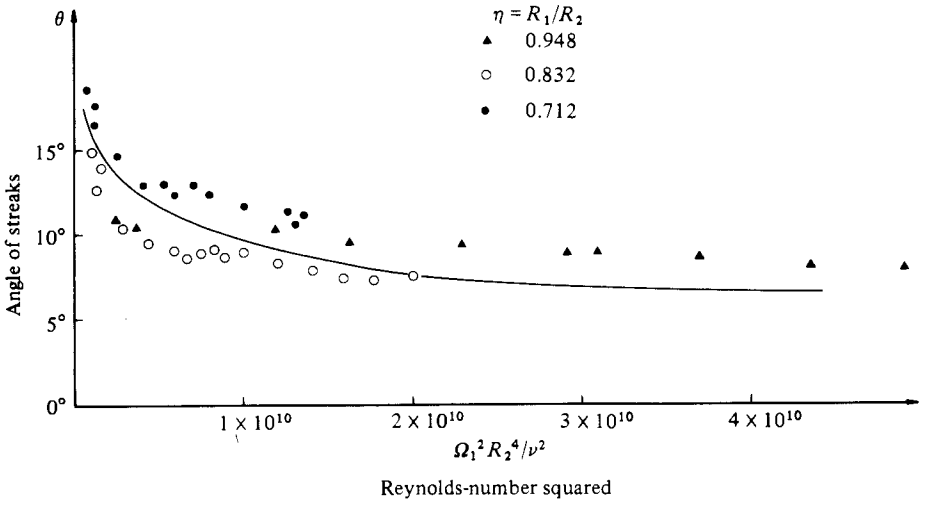

FIGURE 8. Variation with T of orientation of Görtler vortices. Solid line indicates orientation of *total* velocity vector near outer cylinder as deduced from Taylor-vortex-amplitude observations of Bouabdallah & Cognet (1980) and reproduced in figure 4.

required for marginal stability of both Taylor vortices and Görtler vortices, we can consider, in a qualitative way, how the (small) transports of torque achieved by these vortices can act to 'tune' this profile. Suppose, as a consequence of a slightly excessive value of Γ, the amplitude of a Taylor vortex increases from its equilibrium value; this will *increase* θ and *increase* the radius of curvature of the total streamlines near the wall. In the absence of other changes, the Görtler number will be *decreased* and the amplitude of the Görtler vortices will *decrease* in intensity, leading to an imbalance in the torque transport by these vortices. This must be compensated by a small change in the mean profiles in which, since the mean interior profile must transport less torque, the value of Γ will *decrease*. This negative-feedback effect, albeit only part of the complex total physics of the problem, presumably aids the persistence of the stable pattern observed.

Finally, then, it appears that most of the readily observable features of the flow at high Taylor number are reproduced by the model we have proposed. The coexistence of steady flow features on widely differing scales, but exhibiting a strong mutual interdependence is perhaps the most interesting feature of the flow we have described. Such a coexistence is known to exist in many turbulent flows (see e.g. Lumley 1981), though not in as steady and readily reproducible a form as here. It is a question of some importance to discover the extent to which this interdependence relies on the strong constraint imposed by rotational symmetry. There appears to be a distinct possibility that this constraint permits the existence in a steady state of coupling mechanisms between boundary layer and 'mainstream' which in other flows, e.g. turbulent channel flows (Beljaars, Prasad & De Vries 1981), occur in unsteady bursts with only a statistical steadiness. If this is so, the Taylor–Couette experiment may prove a valuable test bed for the development of deeper understanding of boundary-layer–mainstream interactions in other turbulent flows.

Our thanks are due to Frank Mobbs for many invaluable discussions and for making his results available to us. We are grateful also to David Quigley for obtaining the experimental results on the scale and orientation of Görtler vortices, and on torque

transports quoted in the text, to Martin Lessen for earlier stimulating discussions on this problem, and finally to the referees for several useful comments and suggestions. This joint research continues a collaboration which started when one of us (AB) was liaison scientist with ONR, London. ONR partial support (N000-14-78-C-0106) is gratefully acknowledged. This paper is Contribution 182 of the Geophysical Fluid Dynamics Institute, Florida State University.

Appendix. Inclusion of the effects of non-zero Γ

The equations governing the motion on the Taylor-cell scale may be written ((3.14), (3.15), (3.19), (6.4), (6.5), (5.9)) as

$$\left.\begin{aligned} &\nabla^6\tilde{\psi}_1-\lambda\{1+\Gamma(1-2x)\}\tilde{\psi}_{1zz}=0,\\ &\tilde{\psi}_{1xxxx}(0,z)=\tilde{\psi}_{1xxxx}(1,z)=0,\\ &\tilde{\psi}_1(0,z)=\tilde{\psi}_1(1,z)=0,\\ &\tilde{\psi}_{1xx}(0,z)+\frac{2\Gamma}{1-\Gamma}\tilde{\psi}_{1x}(0,z)=0,\\ &\tilde{\psi}_{1xx}(1,z)-\frac{2\Gamma}{1-\Gamma}\tilde{\psi}_{1x}(1,z)=0, \end{aligned}\right\} \tag{A 1}$$

where

$$\lambda = a\Gamma/E_K^2. \tag{A 2}$$

If we now write

$$\left.\begin{aligned} \lambda &= \lambda^{(0)}+\Gamma\lambda^{(1)}+\ldots,\\ \tilde{\psi}_1 &= \tilde{\psi}_1^{(0)}+\Gamma\tilde{\psi}_1^{(1)}+\ldots, \end{aligned}\right\} \tag{A 3}$$

we can establish a sequence of problems at increasing powers of Γ. The zeroth-order problem is of course the classic free–free Rayleigh–Bénard convection problem, as we have observed in §6. The first-order problem becomes

$$\left.\begin{aligned} &\left(\nabla^6-\lambda^{(0)}\frac{\partial^2}{\partial z^2}\right)\tilde{\psi}_1^{(1)}=\lambda^{(1)}\tilde{\psi}_{1zz}^{(0)}+(1-2x)\,\lambda^{(0)}\tilde{\psi}_{1zz}^{(0)},\\ &\tilde{\psi}_{1xxxx}^{(1)}(0,z)=\tilde{\psi}_{1xxxx}(1,z)=0,\\ &\tilde{\psi}_1^{(1)}(0,z)=\tilde{\psi}_1^{(1)}(1,z)=0,\\ &\tilde{\psi}_{1xx}^{(1)}(0,z)=-2\tilde{\psi}_{1x}^{(0)}(0,z),\\ &\tilde{\psi}_{1xx}(1,z)=2\tilde{\psi}_{1x}^{(0)}(1,z). \end{aligned}\right\} \tag{A 4}$$

Equations (A 4) clearly constitute a forced system, and we need to express an orthogonality condition to permit a solution. Multiplying the differential equation of (A 4) throughout by $\tilde{\psi}_1^{(0)}$ and integrating from $x=0$ and $x=1$ then yields a value for $\lambda^{(1)}$.

On assuming that

$$(\tilde{\psi}_1^{(0)},\tilde{\psi}_1^{(1)}) = (F^{(0)}(x),F^{(1)}(x))\cos kz, \tag{A 5}$$

we find, on using the boundary conditions, that the orthogonality condition takes the form

$$[F_{xxx}^{(0)}F_{xx}^{(1)}-3k^2F_x^{(0)}F_{xx}^{(1)}]_0^1=\lambda^{(1)}k^2\langle F^{(0)2}\rangle-\lambda^{(0)}k^2\langle(1-2x)F^{(0)2}\rangle, \tag{A 6}$$

where

$$\langle\ \rangle=\int_0^1 \mathrm{d}x\ (\ ).$$

If we now set

$$F^{(0)}(x) = \sin m\pi x \quad (m = 1, 2, \ldots), \tag{A 7}$$

and note that

$$F^{(1)}_{xx}(0) = -2F^{(0)}_{x}(0)$$

and

$$F^{(1)}_{xx}(1) = 2F^{(0)}_{x}(1),$$

we find finally that

$$\lambda^{(1)} = -8m^2\pi^2(m^2\pi^2 + 3k^2)\, k^{-2}. \tag{A 8}$$

Thus

$$\lambda \approx \{(m^2\pi^2 + k^2)^3 - 8m^2\pi^2\Gamma(m^2\pi^2 + 3k^2)\}/k^2 + \ldots. \tag{A 9}$$

If we now assume that the most-unstable mode is $m = 1$, we find, on minimizing with respect to k, that

$$2k^2 - \pi^2 = -\frac{8\pi^2\Gamma}{(\pi^2 + k^2)^2}, \tag{A 10}$$

whence, writing

$$k^2 = k_0^2 + \Gamma k_1^2 + \ldots, \tag{A 11}$$

we have

$$k_0^2 = \tfrac{1}{2}\pi, \quad k_1^2 = -\frac{32}{9\pi^2}. \tag{A 12}$$

Thus the value of k^2 for the mode going unstable at the lowest value of λ is

$$k^2 = \tfrac{1}{2}\pi^2 - \frac{32\Gamma}{9\pi^2} + O(\Gamma^2);$$

for $\Gamma \approx 0.2$ the correction on the classical value $\frac{1}{2}\pi^2$ is seen to be only about 1.5%.

REFERENCES

Barcilon, A., Brindley, J., Lessen, M. & Mobbs, F. R. 1979 *J. Fluid Mech.* **94**, 453–463.

Batchelor, G. K. 1960 A theoretical model of the flow at speeds far above the critical. Appendix to R. J. Donnelly & H. J. Simon. *J. Fluid Mech.* **7**, 401.

Beljaars, A. C. M., Prasad, K. K. & de Vries, D. A. 1981 *J. Fluid Mech.* **112**, 33–70.

Bippes, H. 1972 In *Sitzungsberichte der Heidelberger Akademie der Wissenschaften Mathematisch-Naturwissenschaftliche Klasse, Jahrgang 1972.*

Blackwelder, R. F. & Eckelmann, H. 1979 *J. Fluid Mech.* **94**, 577–594.

Bouabdallah, A. & Cognet, G. 1980 In *Laminar–Turbulent Transition* (ed. R. Eppler & H. Fasel), p. 368. Springer.

Brindley, J., Mobbs, F. R. & Quigley, D. J. 1981 Paper presented at Taylor Vortex Working Party, Tufts University.

Busse, F. H. 1978 *Adv. Appl. Mech.* **18**, 77–123.

Busse, F. H. 1981 In *Hydrodynamic Instabilities and the Transition to Turbulence* (ed. H. L. Swinney & J. P. Gollub), pp. 97–137. Springer.

Chandrasekhar, S. 1961 *Hydrodynamic and Hydromagnetic Stability.* Oxford University Press.

Di Prima, R. C. & Swinney, H. L. 1981 In *Hydrodynamic Instabilities and the Transition to Turbulence* (ed. H. L. Swinney & J. P. Gollub), pp. 139–180. Springer.

Floryan, J. M. & Saric, W. S. 1982 *AIAA J.* **20**, 316–323.

Görtler, H. 1940 *Nachr. Ges. Wiss. Gött. Math. Phys. Kl.* **1**, 1–26 [translated as *NACA Tech. Memo.* 1375].

Hall, P. 1982 *J. Fluid Mech.* **124**, 475–494.

Hall, P. 1983 *J. Fluid Mech.* **130**, 41–58.

Hammerlin, G. 1956 *Z. angew. Math. Phys.* **7**, 156–164.

Howard, L. N. 1963 *J. Fluid Mech.* **17**, 405–432.

Koschmieder, E. L. 1979 *J. Fluid Mech.* **93**, 515–527.

Lumley, J. L. 1981 In *Transition and Turbulence* (ed. R. E. Meyer). Academic.

MALKUS, W. V. R. 1979 *J. Fluid Mech.* **90**, 401–414.

MEKSYN, D. 1950 *Proc. R. Soc. Lond.* A **203**, 253–265.

MEKSYN, D. 1961 *New Methods in Laminar Boundary Layer Theory.* Pergamon.

SHORT, M. G. & JACKSON, J. H. 1977 In *Superlaminar Flow in Bearings, Proc. 2nd Leeds–Lyon Symp. Tribol.* (ed. D. Dowson, M. Godet & C. M. Taylor), pp. 28–33. Lond. Inst. Mech. Engng.

SMITH, A. M. O. 1955 *Q. Appl. Maths* **13**, 233–262.

SMITH, G. P. & TOWNSEND, A. A. 1982 *J. Fluid Mech.* **123**, 187–218.

TAYLOR, G. I. 1923 *Phil. Trans. R. Soc. Lond.* A **223**, 289–343.

TAYLOR, G. I. 1935 *Proc. R. Soc. Lond.* A **151**, 494–512.

TOWNSEND, A. A. 1976 *The Structure of Turbulent Shear Flow*, 2nd edn. Cambridge University Press.

WATTENDORF, F. L. 1935 *Proc. R. Soc. Lond.* A **148**, 565–598.